Chinese Chemical Letters 35 (2024) 108616

Contents lists available at ScienceDirect

Chinese Chemical Letters

journal homepage: www.elsevier.com/locate/cclet

Photo-manipulated polyunsaturated fatty acid-doped liposomal hydrogel for flexible photoimmunotherapy

Xinyue Lan[a,b,1], Junguang Liang[a,1], Churan Wen[b], Xiaolong Quan[b], Huimin Lin[b], Qinqin Xu[b], Peixian Chen[c], Guangyu Yao[a,*], Dan Zhou[c,*], Meng Yu[b,d,*]

[a] Breast Center, Department of General Surgery, Nanfang Hospital, Southern Medical University, Guangzhou 510515, China
[b] NMPA Key Laboratory for Research and Evaluation of Drug Metabolism & Guangdong Provincial Key Laboratory of New Drug Screening, School of Pharmaceutical Sciences, Southern Medical University, Guangzhou 510515, China
[c] Department of Breast Surgery, The First People's Hospital of Foshan, Foshan 528100, China
[d] Zhujiang Hospital, Southern Medical University, Guangzhou 510282, China

ARTICLE INFO

Article history:
Received 16 April 2023
Revised 23 May 2023
Accepted 25 May 2023
Available online 26 May 2023

Keywords:
Photodynamic therapy
Immunotherapy
Responsive release
Immunogenic cell death
Liposomal hydrogel

ABSTRACT

Despite the synergy of immune checkpoint blockade (ICB) therapy and photodynamic therapy (PDT) holds great promise as countermeasures against breast cancer, exploring long-term or flexible short-time therapeutic strategies in "cold" tumors remains a great challenge. Here, we present a polyunsaturated fatty acid-doped liposomal hydrogel Lp(DHA)@CP Gel loaded with photosensitizer chlorin e6 (Ce6) and programmed death-ligand 1 antibody (αPD-L1) for flexible local photoimmunotherapy with merely single-dosed administration. The presence of polyunsaturated fatty acid (docosahexaenoic acid, DHA) doped in particle membrane endows liposomes with flexibly reactive oxygen species (ROS)-responsive release capability, which was attributed to the presence of abundant unsaturated groups. The αPD-L1 was repeatedly induced to *in situ* release in response to the PDT under photo-exposure. The immunogenic cell death (ICD) effect of PDT evoked "cold" breast tumor to "hot" one, and then assisted the cascade released αPD-L1 to synergistically boost the immunotherapy. After a single dose of peritumoral administration of Lp(DHA)@CP Gel, the on-demand treatment can maximize patient compliance and safety by adjusting therapeutic behaviors *via* a photo on-off switch. This work presents a flexible medication platform, showing promise in improving the objective response rate of ICB therapy and minimizing its systemic toxicity.

Despite significant advances in breast cancer treatment, it is still the major cause of cancer-related death in females worldwide [1]. In recent years, a high-profile treatment, immunotherapy has developed rapidly against tumors [2–4]. Although many clinically used drugs have inhibited tumor growth and metastasis to some extent, most of them hardly achieve long-term or flexible short-time therapeutic effects with merely single-dose administration [5,6]. Hydrogel is composed of crosslinked polymeric networks that can form highly hydrated semisolid materials, which facilitate drug deposition and sustained release [7–9]. With the continuous development of nanotechnology in the past decades, numerous researchers have designed various *in-situ* drug release therapeutic strategies using injectable nanomedicine-loading hydrogels as a drug reservoir [10,11]. For example, Chen has employed a minimal invasiveness measurement to inhibit tumor growth by local injection of programmed death-ligand 1 antibody (αPD-L1) loaded hydrogel [12]. Luo has also reported an all-in-one and all-in-control gel depot to realize a locally symbiotic mild photothermal-assisted immunotherapy [13]. The high peritumoral drug accumulation is beneficial to taking effect, however, the drug release behavior is usually hard to be flexibly adjusted, leading to the unnecessary sustained release of drugs in disease site and accompanied with excessive treatment risks, which are of particular concern in immunotherapy [14,15]. Therefore, the designing of intelligent antitumor platform with high drug storage capability and adjustable release property is highly desirable [16,17].

Recently, hydrogels crosslinked *via* dynamic covalent bonds attracted extensive attention due to their "smart property" originated from the kinetically controlled structures [18–20]. In this situation, it has inspired us to propose the on-demand tumor therapeutic

* Corresponding authors.
E-mail addresses: yaogy@smu.edu.cn (G. Yao), zdan14@fsyyy.com (D. Zhou), yumeng999@smu.edu.cn (M. Yu).
[1] These authors contributed equally to this work.

https://doi.org/10.1016/j.cclet.2023.108616
1001-8417/

hydrogels involving stimuli-responsive drug-carrying nanoparticles to realize the localized accumulation and induced repeated release of drugs, thereby decreasing the administration times and avoiding excessive treatment as well as the accompanied side. Previous studies have confirmed that amphiphilic materials with unsaturated structures undergo reversible hydrophobic-hydrophilic structural transitions induced by reactive oxygen species (ROS), contributing to the ROS-responsive on-demand disassembly and the subsequent cargo release of nanoparticles constructed based on these functional materials [21,22]. In the previous research, we have confirmed that the drug-loaded nanoparticles prepared based on the unsaturated materials, such as lecithin and docosahexaenoic acid (DHA) would be disintegrated in response to the overexpressed intratumoral ROS or highly-produced ROS during photodynamic therapy (PDT) to achieve on-demand drug release. The polyunsaturated fatty acid DHA doped in particle membrane endows liposomes with flexibly ROS-responsive release capability, which was attributed to the presence of abundant unsaturated groups [23]. Therefore, it inspired us to combine ROS-induced reversible immune drug release liposomal gel with PDT to achieve light-triggered and spatio-temporally controlled photodynamic-/immuno-cascade therapy after one-dose administration.

Although immunotherapy represented by immune checkpoint blockade (ICB) strategy has shown outstanding advantages in breast cancer, especially triple-negative breast cancer treatment, it is still facing risks such as drug resistance and recurrence [24–27]. However, most of the breast cancers are considered as immunosuppressive "cold" tumors, which are hyposensitive to ICB therapies due to the insufficient tumor-infiltrating lymphocytes (TILs) and rich tumor-promoting macrophages or regulatory T cells (Tregs), and excessive anti-inflammatory cytokines [28–30]. Many studies have shown that PDT can strengthen ICB therapy by converting a nonimmunogenic "cold" tumor to an immunogenic "hot" tumor [31–33]. The introduction of phototherapy promotes the tumor-associated antigen (TAA) presenting to T cells, activating systemic immune responses thus improving tumor sensitivity to immunotherapy [34,35]. For example, Zhao *et al.* designed an immune-enhancing polymer-reinforced liposome to enhance TAA cross-presentation in dendritic cells (DCs), and then improving the immunogenic cell death (ICD) associated antitumor efficiency by inducing the tumor cells to expose pro-phagocytic calreticulin and release high mobility group box 1 [36]. Therefore, combining ICB therapy with PDT denotes a promising strategy to potentiate the immune therapy by transferring tumor immune environment from "cold" to "hot".

In this work, we fabricated an ROS-responsive liposomal hydrogel loading αPD-L1 (Lp(DHA)@CP Gel) to *in situ* implant in tumor site as a drug depot for repeatedly long-term photoimmunotherapy. The ROS induced by 671 nm laser irradiation led to tumor cell apoptosis through PDT effect, meanwhile, the generated ROS as well causing reversible αPD-L1 release from Lp(DHA)@CP Gel due to the peroxidation of unsaturated membrane materials that lead to disintegrity of liposomes (Scheme 1). Moreover, the immunogenic PDT reversed immune cold tumor into hot one by recruiting effector T cells, and then evoked tumor immunity to assist the cascade released αPD-L1 for synergistic immunotherapy. Notably, Lp(DHA)@CP Gel maximized the synergistic antitumor efficacy on breast tumor-bearing mice by photo-manipulated on-off release of immune drugs. In addition, this flexible medication platform facilitated on-demand photoimmunotherapy as well as greatly avoiding clinical overtreatment risks on patients. In addition, this flexible medication platform facilitates on-demand photoimmunotherapy, significantly avoiding the risk of clinical overtreatment in patients. By reducing the injection times and adjusting therapeutic behaviors *via* a photo on-off switch, the treatment can achieve a high concentration of the drugs in the local tumor microenvironment with lower side effects, which can maximize patient compliance and safety.

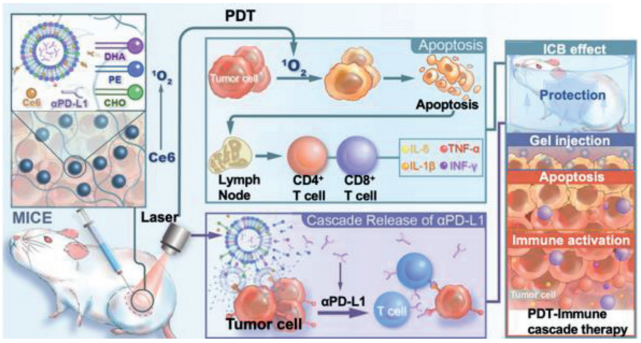

Scheme 1. Schematic illustration of the antitumor mechanism of flexible photoimmunotherapy by Lp(DHA)@CP.

The Lp(DHA)@CP were synthesized by film dispersion method with ROS-responsive polyunsaturated fatty acid DHA doped in the liposomal membrane. Lp(DHA)@CP Gel was then formed by mixing with the same volume of aldehyde-modified xanthan gum. Fig. 1a and Fig. S1 (Supporting information) clearly showed that the Lp(DHA)@CP Gel could be easily extruded through a syringe, and remained immobile and stable in aqueous circumstance. In addition, the hydrogel cut into two pieces could be fused and recovered to a homogeneous gel along the cutting line [37]. The scanning electron microscope (SEM) image shown in Fig. 1b illustrated the morphology of Lp(DHA)@CP Gel and the spherical shaped Lp(DHA)@CP on the surface of hydrogel. The dynamic light scattering (DLS) data and transmission electron microscope (TEM) image confirmed the uniform and nanosized liposomes incorporated in the hydrogel with a particle size of ~228 nm and a polymer dispersity index (PDI) of 0.107 (Fig. 1c).

The dynamic crosslinking hydrogel network of Lp(DHA)@CP Gel attributed to the construction of Schiff base bonds between the hydrophilic amino head group of Lp(DHA)@CP and the aldehyde groups of xanthan gum matrix, facilitated its injectable capability [38]. Therefore, Fourier transformed-infrared (FTIR) spectra of different hydrogels were characterized to evaluate the synthesis of Schiff base bonds (Fig. S2 in Supporting information). The FTIR spectrum of Lp(DHA)@CP Gel showed the disappearance of the peak represented for aldehyde group on xanthan gum (ν(C=O), 1732 cm^{-1}) [39]. In contrast, the DHA-absent liposomal hydrogel Lp@CP Gel remained the representative aldehyde group peak, verified that the formation of Schiff base bond highly depend on the existence of amino groups on DHA. Moreover, the degradation of liposomes after the addition of H_2O_2 did not make any changes of FTIR spectrum, evidenced that the integrity or disassembly of the liposome during the responsive drug release process would not change the hydrogel structure.

The injectable hydrogel was expected to be administrated through a syringe and remained *in situ* to perform long-term therapeutic effect [40]. Therefore, the storage modulus (*G'*) and the loss modulus (*G''*) *versus* frequency were measured to evaluate the viscoelastic property of the hydrogel materials. The *G'* value was much higher than that of *G''* during the stress from 1 Pa to 20 Pa or the sweeps from 0.5 rad/s to 25 rad/s, indicating a representative elastic network in Lp(DHA)@CP Gel (Fig. 1d, Figs. S3 and S4 in Supporting information). As expected, when the stress or frequency increased, the *G'* was decreased much more dramatically than that of *G''*, resulted to an obviously lower *G'* value than *G''*, displaying the typical shear-thinning character. The hydrogel was typical of a well-developed network with good mechanical stability, which was favorable for prolonging the retention time at the injection site.

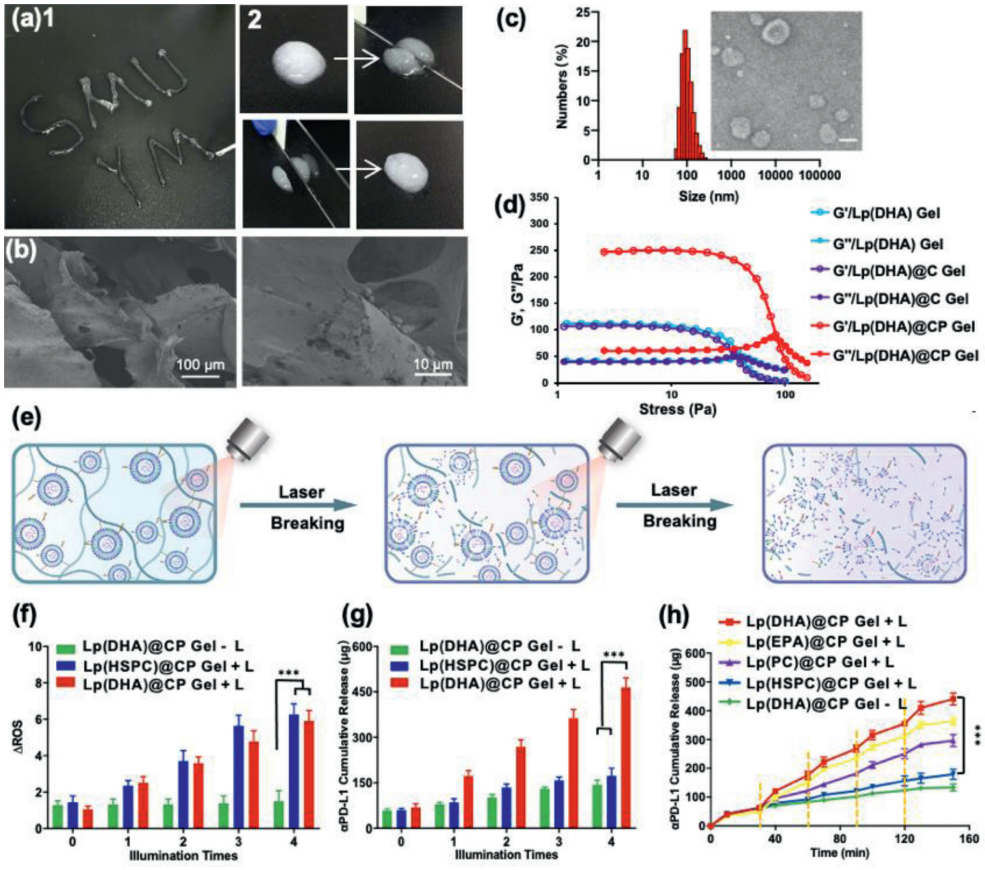

Fig. 1. Synthesis and characterization of the Lp(DHA)@CP Gel. (a) Injectable and self-healing capabilities of the liposomal hydrogel evaluated by extruding through a syringe (1) and cut-recovery study (2). (b) Representative SEM images of the freeze-dried Lp(DHA)@CP Gel. (c) TEM image and particle size distribution of the Lp(DHA)@CP. Scale bar: 200 nm. (d) Storage modulus *G'* and loss modulus *G''* of the Lp(DHA)@CP Gel at different stress at 37 °C. (e) Schematic of photo-triggered cargo release from liposome hydrogels. Cumulative ROS production (f) and corresponding αPD-L1 release (g) from different liposome hydrogels triggered by laser irradiation (671 nm, 100 mW/cm^2, 3 min) for different times. (h) Short-term responsive release of αPD-L1 from liposome hydrogels at 37 °C with and without laser irradiation (671 nm, 100 mW/cm^2, 3 min) at different time points indicated by dotted lines. The error bars indicate means ± standard deviation (SD) ($n = 3$). $^{***}P < 0.001$.

The photosensitizer Ce6 encapsulated in liposomal membrane could be triggered by near-infrared (NIR) laser to mediate the generation of ROS, which would further cause peroxidation of the unsaturated lipid DHA doped in membrane [41,42]. The amphipathic DHA molecule could be reversibly oxidized to a complete hydrophilic structure, therefore destabilized the hydrophobic interaction between amphipathic agents to disturb the integrity of the liposome and then allowed the release of encapsulated cargoes [43]. Hence, the DHA-dependent liposome endowed the Lp(DHA)@CP Gel with the stability in the absence of NIR laser irradiation, meanwhile, the responsive αPD-L1 release property under NIR laser exposure, which process could be repeatedly controlled induced by applying or removing the photosource (Fig. 1e). The overall increased absorption and the characteristic peaks of Ce6 at 404 nm and 280 nm in ultraviolet–visible (UV–vis) spectra provided evidences for the successful construction of Lp(DHA)@CP nanoparticles and the efficient encapsulation of Ce6 (Fig. S5 in Supporting information). Analysis showed that the encapsulation efficiency of Ce6 and αPD-L1 in the liposome was 53.4% ± 1.1% and 65.7% ± 2.1%, respectively. Along with the irradiation time, the absorption peak represented for Ce6 was gradually decreased meanwhile another absorption peak at 238 nm represented for lipid peroxide was obviously increased (Fig. S6 in Supporting information), indicated the formation of the conjugated dienes after the lipid peroxidation process [44].

The responsive generation of ROS upon exposure to NIR light disassembled the liposome structure, which would then trigger a spontaneous cascade reaction to release the interior αPD-L1. To further investigate the mechanism of phototriggered drug release, liposomal hydrogels prepared with saturated (hydrogenated soy phosphatidylcholine (HSPC)) or unsaturated (DHA) lipid materials were to study the ROS generation and αPD-L1 release profiles with or without NIR light irradiation. It was obvious that the liposomal hydrogels were able to produce equivalent ROS amount induced by NIR laser at the same concentration of Ce6 (Fig. 1f). However, only a small portion of αPD-L1 was released from LP(HSPC)@CP Gel triggered by NIR light, while the αPD-L1 release was remarkedly enhanced in LP(DHA)@CP Gel (Fig. 1g), which convinced that the phototriggered drug release property was highly dependent on the existence of ROS-oxidizable unsaturated liposomal membrane materials. This phenomenon was further evidenced by the comparison between liposomal hydrogels with materials of different unsaturation degrees. Amongst, DHA-based liposomal gel has significant higher degree of unsaturation compared to those based on eicosapentaenoic acid (EPA), phosphatidyl choline (PC) and HSPC. No obvious photo-boosted drug release was observed in the saturated HSPC-dependent group, while a significant release inducement was found in monounsaturated EPA and PC groups, and an even more release improvement in polyunsaturated DHA group (Fig. 1h). These results not only illustrated the dependence of photo-responsive drug release on unsaturated materials, but also underlined the positive corresponding relationships between ROS-responsiveness and unsaturation degrees.

The injectable Lp(DHA)@CP Gel showed outstanding advantages in the convenience of clinical application attributed to its repeatedly-induced therapeutics after a single implantation, which

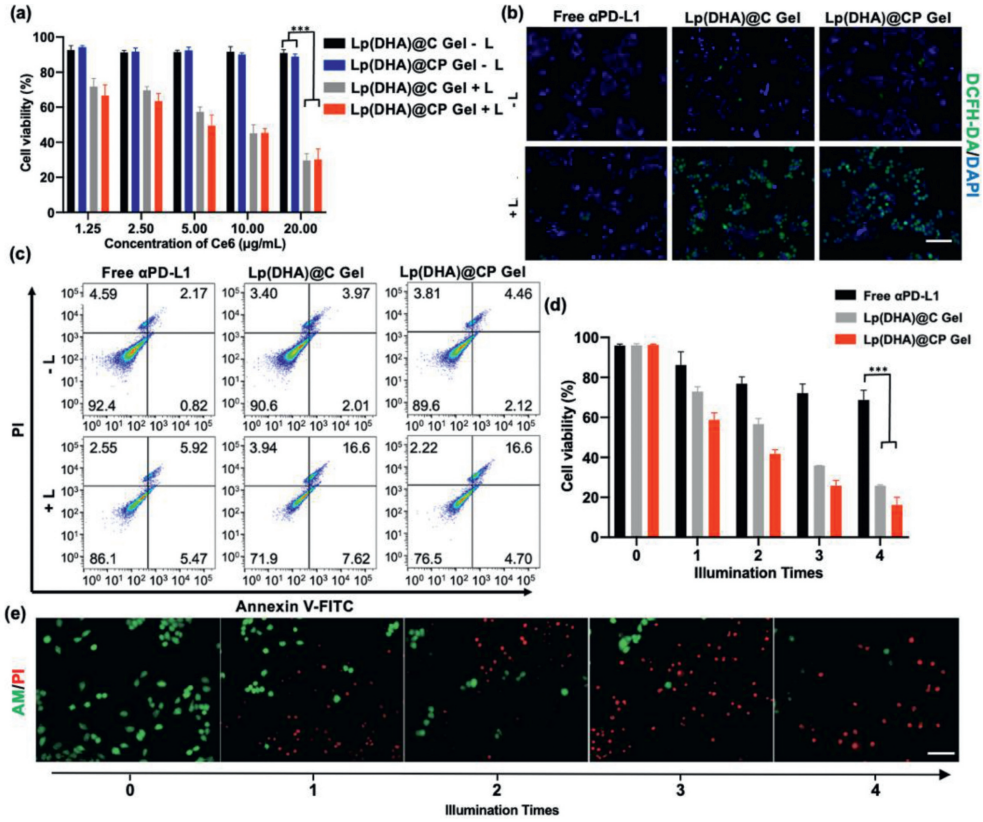

Fig. 2. Photo-triggered cytotoxicity of Lp(DHA)@CP Gel. (a) Cytotoxicity of liposome hydrogels on 4T1 cells with or without laser irradiation (671 nm, 100 mW/cm^2, 3 min). (b) ROS generation in 4T1 cells after different treatments with or without NIR laser irradiation (671 nm, 100 mW/cm^2, 3 min) determined by CLSM observation using DCFH-DA kit. Scale bar: 100 μm. (c) Cell apoptosis of 4T1 cells after different treatments with or without laser irradiation (671 nm, 100 mW/cm^2, 3 min) determined by flow cytometry. (d) Cytotoxicity of hydrogels (concentration of Ce6: 10 μg/mL) on 4T1 cells with laser irradiation (671 nm, 100 mW/cm^2, 3 min) for different times. (e) CLSM observation of photo-triggered cytotoxicity of Lp(DHA)@CP Gel (concentration of Ce6: 10 μg/mL) on 4T1 tumor cells after laser irradiation (671 nm, 100 mW/cm^2, 3 min) for different times. The live and dead cells were stained by calcein AM (green) and propidium iodide (red), respectively. Scale bar: 100 μm. The error bars indicate means ± SD ($n = 3$). $^{***}P < 0.001$.

was beneficial for long-term treatment. As shown in Fig. S7 (Supporting information), Lp(DHA)@CP Gel performed a steady αPD-L1 release after repeatedly triggered for 4 times over 10 d. In order to simulate the intrinsic ROS level in tumor microenvironment and the controlled ROS level by PDT, H_2O_2 with different concentrations rather than irradiation conditions were given to mimic intrinsic intratumoral conditions. The Lp(DHA)@CP Gel showed a relatively stable drug incorporation in the tumor microenvironment-mimic H_2O_2 conditions, while a significant drug release under the laser irradiation (Fig. S8 in Supporting information). Furthermore, despite the gradual release of αPD-L1 once or repeatedly triggered by the laser or H_2O_2, the hydrogel remained stable and reasonable quality loss in aqueous solutions for over 10 d (Figs. S9 and S10 in Supporting information), confirming the excellent stability of Lp(DHA)@CP Gel that met the requirements for the long-term implantable material.

In order to investigate whether the therapeutic effect of the Lp(DHA)@CP Gel would be attenuated during repeated inducement after one-time implantation during the medication period, we have evaluated the photo-responsive cytotoxicity under different illumination times. Ce6 contained hydrogels was demonstrated a significant tumor cell killing effect once triggered by NIR laser attributed to the ROS-generation role of Ce6, however, the addition of αPD-L1 showed negligible cytotoxicity improvement at both conditions with or without laser exposure (Fig. 2a), which can be explained by that the released αPD-L1 took effects by interfering the reaction between immune cells and tumor cells, rather than directly killing tumor cells [45,46]. The intracellular ROS generation in 4T1 cells was then indicated using dichlorofluorescein diacetate (DCFH-DA) for CLSM observation. The great level of ROS was only found in Lp(DHA)@C Gel + L and Lp(DHA)@CP Gel + L groups with laser irradiation, again proved that the existence of both Ce6 and laser exposure were necessary for ROS generation, which displayed the direct role on *in vitro* cytotoxicity (Fig. 2b). The cell apoptosis measured by flow cytometry analysis further confirmed the ROS-dependent tumor cell killing effect (Fig. 2c). The implantable hydrogel was supposed to perform long-term antitumor effect, therefore its cytotoxicity was further assessed under 4 times of 3 min-laser cycles. As shown in Fig. 2d, the cytotoxicity of Lp(DHA)@CP Gel was superimposed with the illumination times, indicating sustained cytotoxicity during the administration process. The live and dead 4T1 cells with Annexin V/propidium iodide (PI) staining shown in Fig. 2e suggested that Lp(DHA)@CP Gel could induce cell death in response to photo-exposure, which could be strengthened by increasing illumination times.

The *in vivo* anticancer efficacy of Lp(DHA)@CP Gel was evaluated on 4T1-luc tumor-bearing BALB/c mice with one-time implantation and repeated photo-inducement treatment process (Fig. 3a). All animal experiments were performed under the guidelines evaluated and approved by the Ethics Committee of Southern Medical University, China. As the luciferase-labeled 4T1-luc tumors monitored in Fig. 3b, the liposome hydrogels (Lp(DHA)@C Gel and Lp(DHA)@CP Gel) without laser irradiation only exhibited a limited inhibition effect on the tumor growth inhibition compared to the control group. Once exposed to the laser, Lp(DHA)@CP Gel + L was performed almost total ablation of tumors attributed to its PDT

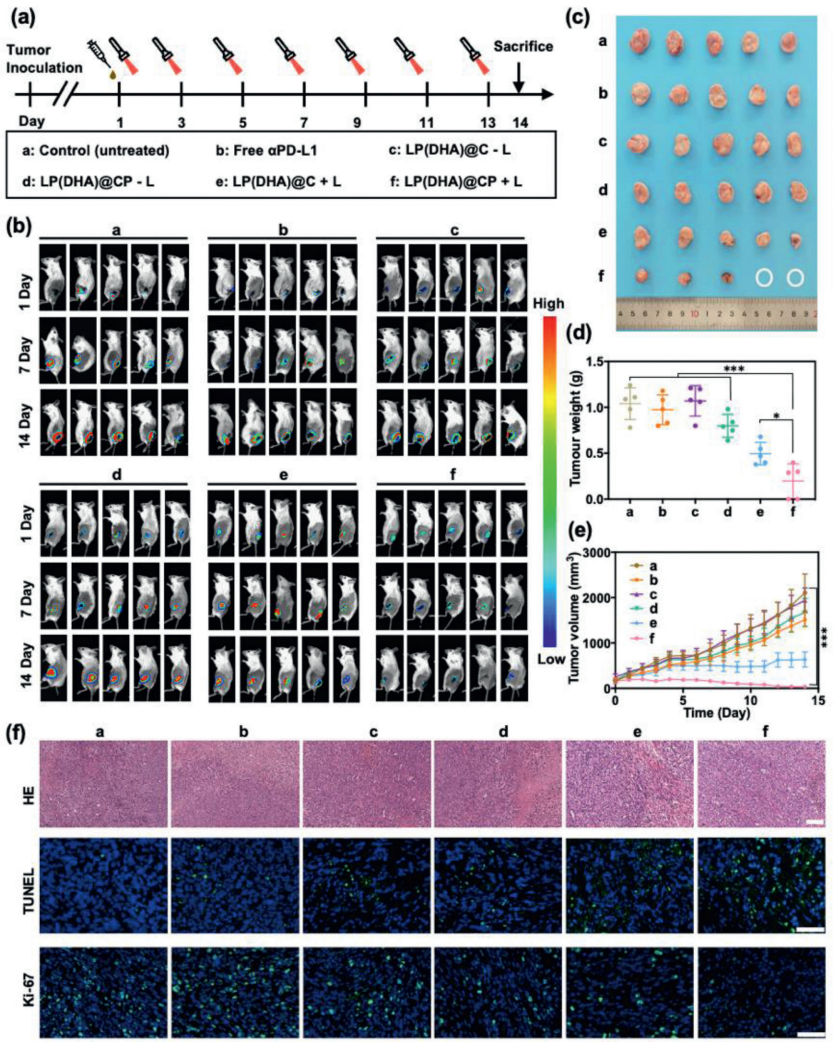

Fig. 3. Antitumor performance of Lp(DHA)@CP Gel by photo-triggering PDT and the cascaded immune therapy effect. (a) Schematic illustration of the antitumor experimental design. (b) Representative *in vivo* bioluminescence images of 4T1 tumor-bearing mice treated with liposome hydrogels at different time points. The photographs (c) and weights (d) of *ex vivo* tumors from different treated mice executed on 14 d (e) average tumor volumes in different groups of 4T1 tumor-bearing BALB/c mice model ($n = 5$). (f) H&E, TUNEL and immunohistochemistry staining of tumor sections from mice receiving various hydrogel-treatments. Scale bar: 100 μm. The error bars indicate means ± SD. $^{*}P < 0.05$, $^{***}P < 0.001$.

effect and the cascaded ICB outcome. The above observations unambiguously evidenced the remarkable sustained anticancer efficacy of the one-time implanted Lp(DHA)@CP Gel repeatedly triggered by laser irradiation.

The individual and average tumor growth curves showed that the Lp(DHA)@CP Gel + L showed a tumor volume increase that was distinctly slower than the other groups (Fig. 3e and Fig. S11 in Supporting information). Amongst, two of the mice even exhibited no measurable tumors at the end of the study (Figs. 3c and d). In addition, no obvious body weight loss was observed in mice treated with each intervention (Fig. S12 in Supporting information). Histological examinations showed no pathological changes in the major organs of mice receiving various treatments (Fig. S13 in Supporting information). Tumor tissues were then harvested and stained with hematoxylin-eosin (H&E) staining and *in situ* terminal deoxynucleotidyl transferase dUTP nick end labeling (TUNEL) for cell morphology observation and apoptosis analysis. According to the histological examinations (Fig. 3f), the most significant classical apoptotic features including condensed and hyperchromatic nuclei were observed in tumor sections from the Lp(DHA)@CP Gel + L, whereas negligible apoptosis was found from the tumors treated with the other interventions. Further TUNEL staining assay confirmed the significantly elevated apoptotic tumor cells in tissues after treated with Lp(DHA)@CP Gel + L. On the other hand, the proliferation of tumor cells after different treatments was also performed by immunofluorescence Ki-67 staining study. As shown in Fig. 3f, obviously decreased Ki-67 positive tumor cells were observed after treated with Lp(DHA)@C Gel + L and Lp(DHA)@CP Gel + L, indicating the potent effects of Ce6-dependent PDT on elevating apoptosis level and suppressing proliferation of tumor cells.

Preclinical studies have shown that local PDT is able to enhance systemic antitumor immunity [47]. The generation of ROS could cause oxidative stress and local inflammation, which is characterized by the rapid influx of $CD8^+$ T cells and $CD4^+$ T cells into the treated tumor bed and an increased expression of proinflammatory cytokines [48,49]. Considering that the efficiency of ICB strategy is severely limited by the low infiltration of effector T cells, PDT could significantly improve the immunotherapy effect of ICB *via* dramatically upregulating intratumoral immune cell infiltration [50]. To further prove the mechanism of synergistic anti-tumor immune therapy mediated by Lp(DHA)@CP Gel + L, the immune responses in tumor tissues after different treatments were further studied. The populations of $CD8^+$ T cells and $CD4^+$ T cells were dramatically increased in Lp(DHA)@C Gel + L and Lp(DHA)@CP Gel + L

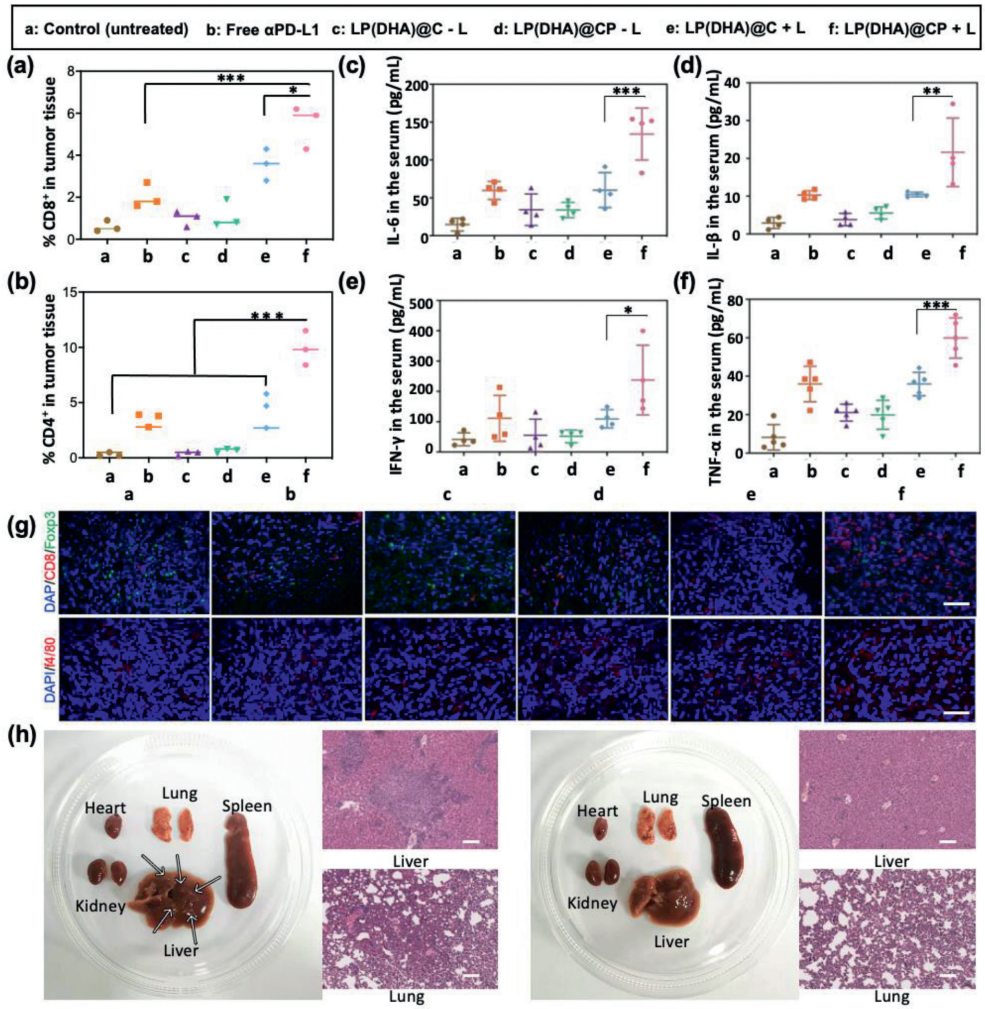

Fig. 4. *In vivo* immune response regulated by Lp(DHA)@CP Gel and long-term anti-metastasis effect. Frequency of tumor-infiltrating $CD8^+$ T cells (a) and $CD4^+$ T cells (b) in the tumor tissues collected from mice after various treatments analyzed by flow cytometry ($n = 3$). Levels of cytokines including IL-6 (c), IL-1β (d), IFN-γ (e) and TNF-α (f) in serum from mice after various treatments measured by ELISA assay. (g) Immunofluorescence assays of $CD8^+$ T cell and macrophages in tumor tissues from mice after various treatments. Scale bar: 100 μm. (h) Long-term anti-metastasis effect of Lp(DHA)@CP Gel evaluated by photographs of major organs and H&E staining of liver and lung sections from 4T1 tumor-bearing mice at 30 d after treatment. Metastatic foci were indicated by arrows. Scale bar: 100 μm. The error bars indicate means ± SD. $^*P < 0.05$, $^{**}P < 0.01$, $^{***}P < 0.001$.

groups (Figs. 4a and b, Fig. S14 in Supporting information), validating the effective immune activation by PDT in tumor microenvironment.

The immune therapy potentiated by PDT not only through recruiting effector T cells, but also mediated *via* modulating macrophages. Interleukin-6 (IL-6) and IL-1β and their downstream mechanisms are involved in a variety of autoimmune inflammatory responses, further affect cell proliferation, differentiation and apoptosis [51]. In addition, a productive T cell response against a tumor antigen results in the upregulated expression of interferon-γ (IFN-γ) in the tumor microenvironment [52], thus the disruption of tumor cell responses to IFN-γ signaling unnecessarily leads to the resistance mechanism to antitumor immunotherapy, including ICB strategy. Therefore, after receiving PDT treatment mediated by Lp(DHA)@C Gel + L or Lp(DHA)@CP Gel + L, the elevated expression of IL-6, IL-1β and IFN-γ in serum released by immune cells for conversely altering T cell responses are the key biomarkers represented for the comprehensive antitumor immune activation (Figs. 4c–e). The immunofluorescence images shown in Fig. 4g again proved the activation of effector T cells and the down-regulation of immunosuppressive Treg cells after the synergistic immunotherapy. Also, the remarkable up-regulation of macrophage infiltration was observed in tumor tissues from mice accepting immune treatments combined with Ce6/laser-dependent PDT. As a positive biomarker that correlates with macrophage infiltration in tumor stroma, tumor necrosis factor-α (TNF-α) secretion was also significantly enhanced after receiving Lp(DHA)@CP Gel + L treatment (Fig. 4f) [53]. The immune activation *via* the recruiting of tumor-inhibiting effector T cell and the suppression of tumor-promoting Treg cells mainly facilitate the long-term tumor inhibition, which was further investigated by the metastasis on the major organs after drug withdrawal (Fig. 4h). The mice treated with Lp(DHA)@CP Gel + L for 2 weeks were kept until 30 d for tumor metastasis monitoring. The liver and lung tissues harvested from mice that received the synergistic immunotherapy showed negligible metastatic foci observed by photographs and H&E staining sections, confirming the anti-metastasis potential of this combined treatment.

In summary, to reduce the medication times and potential overtreatment risks in clinical breast cancer treatment, we have designed a photo-manipulated responsive drug release hydrogel drug delivery platform Lp(DHA)@CP Gel with ROS-responsive disintegrated liposomes cross-linked in it. Abundant ROS was generated by the incorporated Ce6 in response to the NIR light irradiation

for PDT, subsequently mediating the disintegrity of liposomal hydrogel for on-demand sustainable release of αPD-L1. Additionally, the generated ROS in TME was also able to sensitize the low-immunogenic "cold" tumors to "hot" by enhancing the T cell infiltration in tumors, thereby increasing their potential responses to ICB drugs. The injected Lp(DHA)@CP Gel completely inhibited the 4T1 tumor growth, and also restrained the recurrence and metastasis of residual tumors. Therefore, the flexible medication platform facilitated repeated photoimmunotherapy after a single dose administration, maximizing patient compliance and safety by reducing the injection times and adjusting therapeutic behaviors *via* a photo on-off switch.

Declaration of competing interest

The authors declare that they have no known competing financial interests or personal relationships that could have appeared to influence the work reported in this paper.

Acknowledgments

This work was supported by the Natural Science Foundation of Guangdong Province (No. 2023A1515030291), Science and Technology Program of Guangzhou (No. 202201011130280065), National Natural Science Foundation of China (No. 82172079), Special Fund of Foshan Climbing Peak Plan (No. 2020B018).

Supplementary materials

Supplementary material associated with this article can be found, in the online version, at doi:10.1016/j.cclet.2023.108616.

References

[1] H. Sung, J. Ferlay, R.L. Siegel, et al., CA Cancer J. Clin. 71 (2021) 209–249.
[2] H. Zhao, J. Xu, Y. Li, et al., ACS Nano 13 (2019) 13127–13135.
[3] L.Q. Fu, X.B. Ma, Y.T. Liu, et al., Chin. Chem. Lett. 33 (2022) 1718–1728.
[4] D. Wang, T. Nie, C. Huang, et al., Small 18 (2022) e2203227.
[5] J.F. Zirkelbach, M. Shah, J. Vallejo, et al., J. Clin. Oncol. 40 (2022) 3489–3500.
[6] M. Yi, X. Zheng, M. Niu, et al., Mol. Cancer. 21 (2022) 28.
[7] A.S. Hoffman, Adv. Drug Deliv. Rev. 54 (2002) 3–12.
[8] Y.K. Li, H.Y. Zheng, Y.X. Liang, et al., Chin. Chem. Lett. 33 (2022) 5030–5034.
[9] S. Correa, A.K. Grosskopf, H.L. Hernandez, et al., Chem. Rev. 121 (2021) 11385–11457.
[10] E. McAlister, B. Dutton, L.K. Vora, et al., Adv. Healthc. Mater. 10 (2021) e2001256.
[11] G. Gao, Y.W. Jiang, H.R. Jia, et al., Biomaterials 188 (2019) 83–95.
[12] M. Chen, Y. Tan, Z. Dong, et al., Nano Lett. 20 (2020) 6763–6773.
[13] L. Huang, Y. Li, Y. Du, et al., Nat. Commun. 10 (2019) 4871.
[14] H. Cabral, H. Kinoh, K. Kataoka, Acc. Chem. Res. 53 (2020) 2765–2776.
[15] F. Wang, H. Su, R. Lin, et al., ACS Nano 14 (2020) 10083–10094.
[16] P.K. Xin, S.Y. Han, J. Huang, et al., Chin. Chem. Lett. 34 (2023) 108125.
[17] G.T. Liu, Y. Zhou, Z.J. Xu, et al., Chin. Chem. Lett. 34 (2023) 107705.
[18] V. Yesilyurt, A.M. Ayoob, E.A. Appel, et al., Adv. Mater. 29 (2017) 1605947.
[19] V.G. Muir, J.A. Burdick, Chem. Rev. 121 (2021) 10908–10949.
[20] Y. Xu, H. Chen, Y. Fang, J. Wu, Adv. Healthc. Mater. 11 (2022) e2200494.
[21] K.T. Magar, G.F. Boafo, X.T. Li, et al., Chin. Chem. Lett. 33 (2022) 587–596.
[22] H. Xu, P. She, B. Ma, et al., Biomaterials 288 (2022) 121734.
[23] Q. Xu, G. Chen, G. Chen, et al., J. Control. Release 347 (2022) 389–399.
[24] I.S. Kim, Y. Gao, T. Welte, et al., Nat. Cell Biol. 21 (2019) 1113–1126.
[25] S. Adams, M.E.G. Mays, K. Kalinsky, et al., JAMA Oncol. 5 (2019) 1205–1214.
[26] A. Bassez, H. Vos, L.V. Dyck, et al., Nat. Med. 27 (2021) 820–832.
[27] E. Masoumi, S.T. Hajghorbani, L. Jafarzadeh, et al., J. Control. Release 340 (2021) 168–187.
[28] S. Wang, Z. Wang, Z. Li, et al., Adv. Healthc. Mater. 11 (2022) e2201240.
[29] T. Wang, Z. Gao, Y. Zhang, et al., J. Control. Release 351 (2022) 272–283.
[30] Y. Zhang, S. Tian, L. Huang, et al., Nat. Commun. 13 (2022) 4553.
[31] L.Z. He, T.Q. Nie, X.J. Xia, et al., Adv. Funct. Mater. 29 (2019) 1901240.
[32] J. Zhang, D. Huang, P.E. Saw, et al., Trends Immunol 43 (2022) 523–545.
[33] M.F. Attia, N. Anton, J. Wallyn, et al., J. Pharm. Pharmacol. 71 (2019) 1185–1198.
[34] V. Sunil, J.H. Teoh, B.C. Mohan, et al., J. Control. Release 350 (2022) 215–227.
[35] R. Guo, S. Wang, L. Zhao, et al., Biomaterials 282 (2022) 121425.
[36] Y. Zhao, Z. Chen, Q. Li, et al., Adv. Funct. Mater. 32 (2022) 2209711.
[37] C.T. Huynh, M.K. Nguyen, D.S. Lee, Chem. Commun. 48 (2012) 10951–10953.
[38] H. Tan, C.R. Chu, K.A. Payne, et al., Biomaterials 30 (2009) 2499–2506.
[39] H.Y. Zhang, X.Y. Yong, J.Y. Zhou, et al., ACS Appl. Mater. Interfaces 8 (2016) 2753–2763.
[40] Y. Ma, J. Yang, B. Li, et al., Polym Chem. 7 (2016) 2037–2044.
[41] B. Halliwell, S. Chirico, Am. J. Clin. Nutr. 57 (1993) 715S–725S.
[42] Y. Zhou, F. Tong, W.L. Gu, et al., Acta Pharm. Sin. B 12 (2022) 1416–1431.
[43] Y. Wang, H. Xu, X. Zhang, Adv. Mater. 21 (2009) 2849–2864.
[44] J. Kiwi, V. Nadtochenko, J. Phys. Chem. B 108 (2004) 17675–17684.
[45] H.Z. Xu, T.F. Li, Y. Ma, et al., Biomaterials 290 (2022) 121833.
[46] C.J. Liu, M. Schaettler, D.T. Blaha, et al., Neuro. Oncol. 22 (2020) 1276–1288.
[47] S.O. Gollnick, J. Natl. Compr. Cancer Netw. 10 (2012) S40–S43.
[48] Y.Y. Xu, J.Y. Xiong, X.Y. Sun, H.L. Gao, Acta Pharm. Sin. B 12 (2022) 4327–4347.
[49] R. Mahjub, S. Jatana, S.E. Lee, et al., J. Control. Release 288 (2018) 239–263.
[50] M. Firczuk, D. Nowis, J. Gołąb, Photochem. Photobiol. Sci. 10 (2011) 653–663.
[51] L.D. Church, G.P. Cook, M.F. McDermott, Nat. Clin. Pract. Rheumatol. 4 (2008) 34–42.
[52] A. Kalbasi, A. Ribas, Nat. Rev. Immunol. 20 (2020) 25–39.
[53] Y. Qiu, T. Chen, R. Hu, et al., Biomark. Res. 9 (2021) 72.